

Photodisintegration of the p-nuclei ^{92}Mo and ^{144}Sm in the astrophysically relevant energy window

C. Nair^{*a}, M. Erhard^a, A. R. Junghans^a, D. Bemmerer^a, R. Beyer^a, E. Grosse^{a,b}, J. Klug^{a†}, K. Kosev^a, G. Rusev^{a‡}, K. D. Schilling^a, R. Schwengner^a and A. Wagner^a

^a*Institut für Strahlenphysik, Forschungszentrum Dresden-Rossendorf, D-01314 Dresden, Germany*

^b*Institut für Kern- und Teilchenphysik, Technische Universität Dresden, D-01062 Dresden, Germany*

E-mail: chithra.nair@fzd.de

The heavy neutron deficient p-nuclei are produced in explosive stellar environments via photodisintegration reactions like (γ, n) , (γ, p) and (γ, α) on r- or s- seed nuclei. The reaction rates of p-nuclei are mostly based on theoretical parameterizations using statistical model calculations. We study experimentally the photodisintegration rates of heavy nuclei at the bremsstrahlung facility of the superconducting electron accelerator ELBE of FZ Dresden-Rossendorf. Photoactivation measurements on the astrophysically relevant p-nuclei ^{92}Mo and ^{144}Sm have been performed with bremsstrahlung end-point energies from 10.0 to 16.5 MeV. The activation yields are compared with calculations using cross sections from recent Hauser-Feshbach models. The sensitivity of the statistical models to the input ingredients like photon strength function, optical potentials are tested against the experimental activation yield.

*10th Symposium on Nuclei in the Cosmos
July 27 - August 1 2008
Mackinac Island, Michigan, USA*

^{*}Speaker.

[†]Present address: Ringhals Nuclear Power Plant, SE-43022 Väröbacka, Sweden

[‡]Present address: Department of Physics, Duke University, Triangle Universities Nuclear Laboratory, Durham, NC 27708, USA.

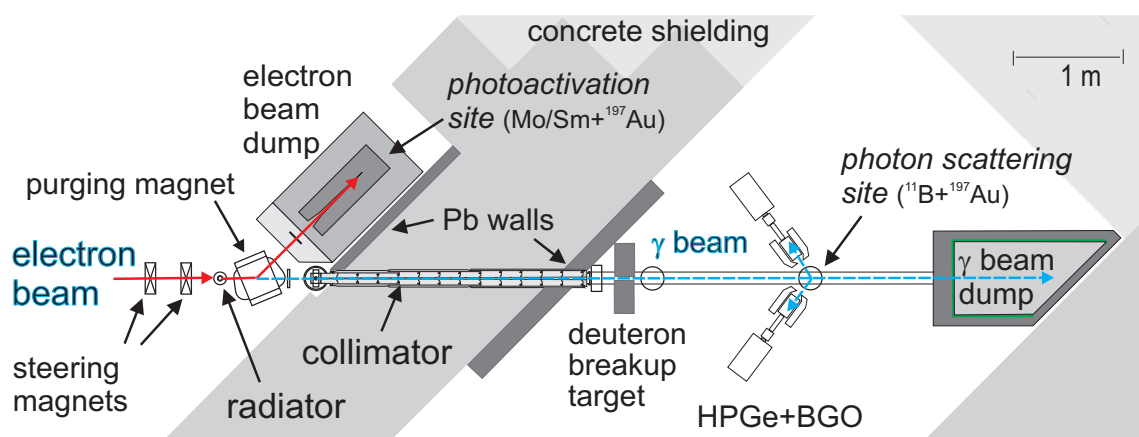


Figure 1: Photoactivation setup at ELBE accelerator [6]. The electron beam is deflected from the main beam line and creates bremsstrahlung in the radiator. There are two target sites: at the photoactivation site, the Mo and/or Sm targets are irradiated together with ^{197}Au as a reference. At the photon scattering site, the scattered photons from ^{11}B are observed for the experimental determination of the flux. Another ^{197}Au target is sandwiched with ^{11}B for flux normalization purposes.

1. Introduction

Most of the nuclei heavier than iron are synthesized mainly by the slow neutron capture process (s-process) or rapid neutron-capture reactions (r-process). However, some stable proton-rich isotopes between Se and Hg are shielded from the rapid neutron capture by stable isobars and are believed to be synthesized by chains of photodisintegrations like (γ, n) , (γ, p) and/or (γ, α) on r- or s- seed nuclei. These are classically referred to as the *p*-nuclei. An overview on *p*-nuclei studies performed so far has been given in [1].

The current *p*-nucleosynthesis modeling is mostly based on theoretical statistical model calculations. With our experiments with real photons, we aim to test the inputs to statistical model calculations. This is particularly important for nuclei like ^{92}Mo which are significantly underproduced in network calculations. In the present paper, we focus on the results from photodisintegration studies of the *p*-nuclei ^{92}Mo and ^{144}Sm . The (γ, n) , (γ, p) and (γ, α) reactions on both nuclei have been performed via the photoactivation technique. The bremsstrahlung endpoint energies for the measurements range from 10.0 to 16.5 MeV. The $^{197}\text{Au}(\gamma, n)$ reaction has been used as an activation standard [2]. Preliminary results have been presented in Refs. [3, 4, 5].

2. Photoactivation method

At the bremsstrahlung facility of the superconducting electron accelerator ELBE (Electron Linear accelerator of high Brilliance and low Emittance) of FZ Dresden-Rossendorf [6], energies up to 20 MeV with average currents up to 1 mA are available which is appropriate for probing photon-induced reactions. The setup has been extensively used for photon scattering as well as photoactivation studies [7, 8, 9]. During the experiments, energy drifts of the electron linac have been stabilized and kept to about 1% using a beam-stabilization control loop.

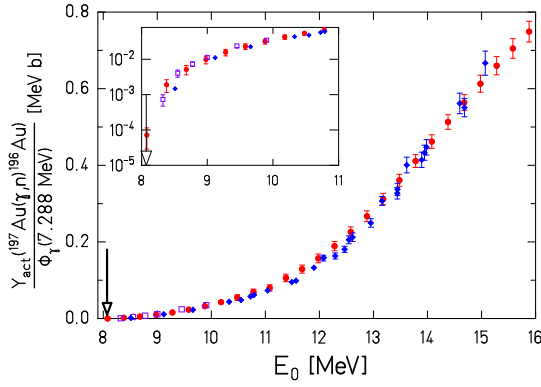


Figure 2: Activation yield for the $^{197}\text{Au}(\gamma, n)$ reaction normalized to the photon fluence is compared to the yield calculated using cross sections measured in previous experiments. The present data are denoted by diamonds with an arrow pointing to the neutron emission threshold. Reaction yield calculated using the cross sections given by Veyssiere et al. [13] (circles) and Vogt et al. [14] (open squares) is in good agreement with the yield measured at ELBE.

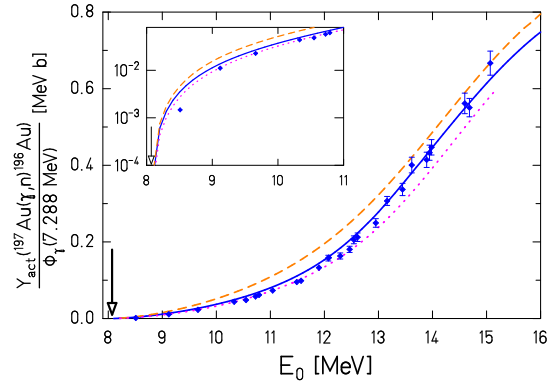


Figure 3: Experimental activation yield normalized to the photon fluence for the $^{197}\text{Au}(\gamma, n)$ reaction compared to theoretical model calculations. The experimental data are denoted by diamond symbols with a downward arrow denoting the neutron emission threshold. The dashed and dotted lines denote yield calculations using cross sections from TALYS [15] and NON-SMOKER [16] code respectively. The solid line represents a TALYS calculation with modified inputs for the photon strength function, see text.

As shown in the schematic sketch (Fig. 1), the primary electron beam is focused onto a thin niobium radiator foil which produces bremsstrahlung via deceleration of electrons. Behind the radiator, the electrons are deflected by a dipole magnet and dumped to the electron beam dump (*photoactivation site*). The photoactivation target (Mo/Sm) is irradiated here together with the activation standard target ^{197}Au . The bremsstrahlung beam goes straight ahead through the collimator to the *photon scattering site*.

In order to determine the photoactivation yield for Mo/Sm, it is necessary to know the absolute photon flux at the photoactivation site. At this high flux area where the flux is nearly 50-100 times higher than the photon scattering site, it is technically not possible to measure the photon flux directly. The photon flux is determined from the activation yield of a Au sample that is irradiated simultaneously with the Mo/Sm samples. The photon flux at a fixed energy E_γ is given by the ratio of the measured Au activation yield and the calculated activation yield using the known $\sigma_{\gamma, n}$ from ^{197}Au and a simulated bremsstrahlung spectrum using the code MCNP [10], which is based on the bremsstrahlung cross sections by Seltzer and Berger [11]. At the photon scattering site, the activation yield of $^{197}\text{Au}(\gamma, n)$ was determined to verify the $\sigma_{\gamma, n}$ cross section to be used for the photon flux determination. There the flux is determined via photon scattering from ^{11}B . Details can be found in our recent paper [2].

After irradiation, decay of the daughter nuclei resulting from photoactivation are measured with HPGe detectors with relative efficiency 90% or 60%. In case that the resulting radioactive nuclei are short-lived, a rapid transport system (rabbit system) was used for measurement (see Sec. 3, Ref. [5]). The measurements demanding low background were performed at the underground laboratory 'Felsenkeller' [12] where 98% of cosmic muons are shielded by the 47 m thick rock

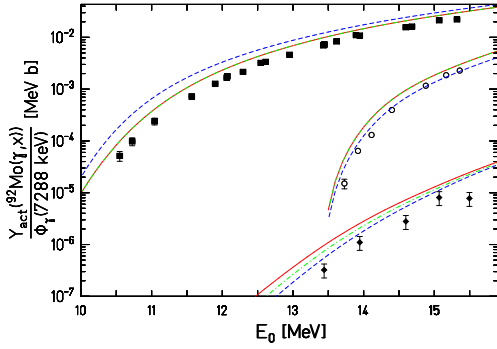


Figure 4: Experimental activation yield normalized to the photon fluence for photodisintegration reactions in ^{92}Mo . For ^{92}Mo , the $^{92}\text{Mo}((\gamma,p)+(\gamma,n))$ (squares), $^{92}\text{Mo}((\gamma,n))$ (open circles) and $^{92}\text{Mo}(\gamma,\alpha)$ (diamonds) yields are shown. The different lines are the yields calculated using TALYS [15] code with Koning-Delaroche (solid line), McFadden and Satchler (dash-dotted) and Jeukenne-Lejeune-Mahaux (dashed) models for the optical model potentials, see text.

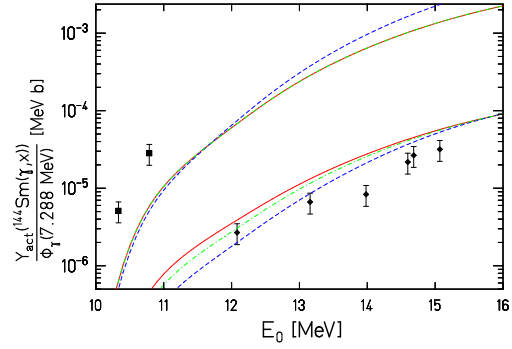


Figure 5: Experimental activation yield normalized to the photon fluence for photodisintegration reactions in ^{144}Sm . The yields for $^{144}\text{Sm}(\gamma,p)$ (squares) and $^{144}\text{Sm}(\gamma,\alpha)$ (diamonds) are shown. The different lines are the yields calculated using TALYS [15] code with Koning-Delaroche (solid line), McFadden and Satchler (dash-dotted) and Jeukenne-Lejeune-Mahaux (dashed) models for the optical model potentials, see text.

layer.

The formulas for determining the activation yield Y_{act} have been explained in detail under Sec. 4 of Ref. [5]. With the known bremsstrahlung spectrum and the experimental photon flux, the activation yield can be calculated from $\sigma_{\gamma,n}(E)$ data. In this way measured activation yields are compared with the experimental or theoretical cross section data.

3. Experimental results

The photoactivation yield for $^{197}\text{Au}(\gamma,n)$ reaction is compared to the yield calculated using cross sections from previous experiments (Fig. 2) as well as using cross sections from statistical models (Fig. 3). The experimental activation yield is in good agreement with the calculated yields using cross sections determined with quasimonoenergetic photons from positron annihilation experiments of Veysiere et al. [13] and also with bremsstrahlung data below 10.0 MeV by Vogt et al. [14]. The activation yield has been compared to the calculated yields based on the model codes TALYS [15] and NON-SMOKER [16]. The experimental data are quite sensitive to the photon strength function (PSF). They are best explained by our proposed new parametrization for the PSF that describes both spherical, deformed and also triaxial nuclei from $A=80-200$ with a spreading width Γ that neither depends on temperature nor on γ energy [2].

The activation yields normalized to the photon fluence for photodisintegration reactions in ^{92}Mo and ^{144}Sm are given in Figs. 4 and 5. The sensitivity of the statistical model code TALYS to the use of different optical model potentials (OMP) is illustrated. The different models being used are the Koning-Delaroche [17], McFadden and Satchler [18] and the semi-microscopic model Jeukenne-Lejeune-Mahaux (JLM [19]). The sensitivity to the OMP is not as large as to the PSF. The JLM parametrisation seem to favor proton emission over neutron emission, while the alpha

emission is reduced. The influence of the alpha-nucleus potential on the activation yield is below a factor of 2.

In brief, the measured activation yields for (γ,n) , (γ,p) and/or (γ,α) in the energy range of the Giant Dipole Resonance (10-16 MeV) indicate that the underproduction of Mo in the p-process nucleosynthesis is likely *not* due to wrong photodisintegration rates in the theoretical calculations. The experimental activation yields for the p-nuclei mentioned here are sensitive to the PSF, whereas the sensitivity to the OMP models is smaller than a factor of 2.

4. Acknowledgements

We thank the ELBE team for providing a stable beam during activation experiments and A. Hartmann for technical assistance. Special thanks are to J. Claussner and his co-workers for building the rabbit system and M. Koehler, D. Degering for the measurements at 'Felsenkeller'.

References

- [1] M. Arnould and S. Goriely, *Physics Reports* **384**, 1 (2003).
- [2] C. Nair *et al.*, Submitted to *Phys. Rev. C*.
- [3] M. Erhard, A. R. Junghans, R. Beyer *et al.*, *European Physical Journal A* **27**, s01 135 (2006).
- [4] M. Erhard *et al.*, *PoS (NIC-IX) 056* (2006).
- [5] C. Nair, A. R. Junghans, M. Erhard *et al.*, *Journal of Physics G-Nuclear and Particle Physics* **35**, 014036 (2008).
- [6] R. Schwengner, R. Beyer, F. Dönau *et al.*, *Nuclear Instruments and Methods A* **555**, 211 (2005).
- [7] R. Schwengner, G. Rusev, N. Benouaret *et al.*, *Physical Review C* **76**, 034321 (2007).
- [8] A. Wagner, R. Beyer, M. Erhard *et al.*, *Journal of Physics G-Nuclear and Particle Physics* **35**, 014035 (2008).
- [9] G. Rusev, R. Schwengner, F. Dönau *et al.*, *Physical Review C* **77**, 064321 (2008).
- [10] MCNP - Monte Carlo N-Particle Transport Code, <http://mcnp-green.lanl.gov/>.
- [11] S. M. Seltzer and M. J. Berger, *Atomic Data and Nuclear Data Tables* **35**, 345 (1986).
- [12] S. Niese, M. Koehler and B. Gleisberg, *Journal of Radioanalytical and Nuclear Chemistry* **233**, 16 (1998).
- [13] A. Veyssiere, H. Beil, R. Bergere *et al.*, *Nuclear Physics A* **159**, 561 (1970).
- [14] K. Vogt, P. Mohr, M. Babilon *et al.*, *Nuclear Physics A* **707**, 241 (2002).
- [15] A. J. Koning, S. Hilaire and M.C. Duijvestijn, *Proceedings of the International Conference on Nuclear Data for Science and Technology - ND2004*, AIP vol. 769, eds. R.C. Haight, M.B. Chadwick, T. Kawano, and P. Talou, Sep. 26 - Oct. 1, 2004, Santa Fe, USA, p. 1154 (2005); <http://www.talys.eu>.
- [16] T. Rauscher and F. K. Thielemann, *Atomic Data and Nuclear Data Tables* **88**, 1 (2004).
- [17] A. J. Koning and J. P. Delaroche, *Nucl. Phys. A* **713**, 231 (2003).
- [18] L. McFadden, G.R. Satchler, *Nucl. Phys.* **84** 177 (1966).
- [19] E. Bauge, J. P. Delaroche, M. Girod, *Phys. Rev. C* **63**, 024607 (2001).